INFECTION AND IMMUNITY, Jan. 1999, p. 308–318 Vol. 67, No. 1
0019-9567/99/$04.00+0

Influence of Acute-Phase Parasite Load on Pathology, Parasitism, and Activation of the Immune System at the Late Chronic Phase of Chagas' Disease

CLAUDIO R. F. MARINHO,[1] MARIA REGINA D'IMPÉRIO LIMA,[1] MARCOS G. GRISOTTO,[2] AND JOSÉ M. ALVAREZ[1]*

Department of Immunology[1] and Department of Parasitology,[2] Instituto de Ciências Biomédicas, Universidade de São Paulo, São Paulo, SP, Brazil

Received 9 July 1998/Returned for modification 18 August 1998/Accepted 23 October 1998

To obtain low and high parasite loads in the acute phase of Chagas' disease, A/J mice were infected with 10^3 or 10^5 *Trypanosoma cruzi* trypomastigotes of the Y strain and treated on day 6 with benznidazol. One year later, chronically infected mice were screened for subpatent parasitemias, tissue pathology, and immune response. Mice infected with the high parasite inoculum showed higher levels of chronic parasitemias, heart and striated muscle inflammation, and activation of the immune system than did mice infected with the low inoculum. Concerning the activation of the immune system, the main findings for high-dose-infected mice were (i) increased numbers of splenocytes, with preferential expansion of $CD8^+$ and $B220^-$ $CD5^-$ cells, many of them bearing a macrophage phenotype; (ii) higher frequencies of B ($B220^+$), $CD4^+$, and $CD8^+$ large lymphocytes; (iii) a shift of $CD4^+$ cells towards a $CD45RB^{Low}$ phenotype; (iv) increased frequencies of both $CD45RB^{Low}$ and $CD45RB^{High}$ large $CD4^+$ cells; (v) augmented numbers of total immunoglobulin (Ig)-secreting cells, with predominance of IgG2a-producing cells; and (vi) increased production of gamma interferon and interleukin 4. In addition, these mice presented lower IgM and higher IgG2a and IgG1 parasite-specific serum antibody levels. Our results indicate that the parasite load at the acute phase of *T. cruzi* infection influences the activation of the immune system and development of Chagas' disease pathology at the late chronic phase of the disease.

In Chagas' disease, individuals who survive the acute phase of *Trypanosoma cruzi* infection develop a parasite-specific immune response that efficiently reduces parasite levels in the tissues and blood. Many different cell types and soluble molecules participate in the control of parasite numbers. Mice lacking B cells (33) or helper (34, 35) or cytotoxic T cells (34, 41, 43) and mice expressing low or no gamma interferon (IFN-γ), interleukin 12 (IL-12), tumor necrosis factor alpha, or granulocyte-macrophage colony-stimulating factor activities are highly susceptible to infection (1, 2, 28, 29, 37, 45). The major protective role of IFN-γ suggests that parasite control is dependent on activation of the Th1 pathway of the immune response. In spite of the protective role of the immune system, however, a small number of *T. cruzi* parasites persist in tissues during the host life span and occasionally gain access to the blood.

At the late chronic phase of the disease, a fraction of infected individuals (10 to 20%) develop clinical symptoms of an inflammatory response-mediated destruction of the heart and/or digestive tract tissues (24). The pathogenesis of the chronic disease, however, is still under debate. The presence of a low number of parasites close to the lesions suggests that host cell destruction could be mediated by self-reactive clones triggered by the (i) persistence of local inflammatory responses, (ii) intense polyclonal lymphocyte activation at the acute phase of infection (22, 23, 47), or (iii) cross-reactivity between parasites and organ-specific self antigens (7, 36). Alternatively, chronic lesions could be generated by continuous destruction of infected tissue by *T. cruzi* and *T. cruzi*-induced inflammatory responses mediated by parasite-specific lymphocytes (42).

Higuchi et al. (15) showed that, in humans, the intensity of chronic myocarditis directly correlates with the level of parasite antigens in the heart. Moreover, Jones et al. (17) and Vago et al. (46) detected *T. cruzi* DNA only in those organs displaying severe pathology. Recently, Tarleton et al. (44) showed that neonatal hearts transplanted into mice chronically infected with *T. cruzi* do not exhibit any significant inflammatory response unless they are directly injected with live parasites. These results indicate that, whatever the mechanism involved in host cell destruction, the presence of parasites has a crucial role in the development of chronic Chagas' disease pathology. The aim of the present work is to determine if the parasite load during the acute phase of *T. cruzi* infection affects the parasitemia, pathology, and immune response at the chronic phase of the disease. One year after infection, we performed a multiparametric analysis of chronically infected mice subjected to different parasite loads at the acute phase of the infection. Then, we individually correlated parasitemias, heart and striated muscle pathology, and different parameters associated with the activation of the immune system. This study leads to the possibility that Chagas' disease pathology could be reduced by therapeutic protocols that control the acute parasite load.

MATERIALS AND METHODS

Mice and parasites. Six- to eight-week-old A/J female mice were obtained from our animal facilities (Biotério de Camundongos Isogênicos, ICB/USP, São Paulo, Brazil). *T. cruzi* parasites of the Y strain were maintained by weekly passages in A/J mice.

Infection and chemotherapy treatment. Mice were infected intraperitoneally (i.p.) with either a low dose (10^3 blood forms) or a high dose (10^5 blood forms) of *T. cruzi* parasites. Six days later, infected or control mice were treated with a

* Corresponding author. Mailing address: Departamento de Imunologia, ICB, Av. Prof. Lineu Prestes, 1730, Universidade de São Paulo, São Paulo, SP, CEP-05508-900, Brazil. Phone: (55) (11) 818 7389. Fax: (55) (11) 818 7224. E-mail: jmamosig@biomed.icb2.usp.br.

single oral dose of benznidazole (Rochagan; Roche) of 1 g/kg of body weight. After a year, mice were bled under ether anesthesia and sacrificed for collection of spleen, heart, and striated muscle.

Screening of parasitemias. In the acute phase of infection, parasitemias were determined by microscopic examination of 5-μl blood samples collected from the tail vein with a heparinized capillary tube as described elsewhere (18). Chronic-phase parasitemias were screened by a semiquantitative subinoculation technique (3). Briefly, aliquots (0.1 ml) of citrated-treated blood from each chronically infected animal were transfused into three naive mice, which received a single i.p. dose of cyclophosphamide 2 days later (Enduxan; Abbott, São Paulo, Brazil; 200 mg/kg of body weight). In the following days, blood-transfused animals were screened for parasitemia by direct microscopic examination. A chronically infected mouse was considered parasitemia positive when yielding at least one positive sample. Parasitemia levels were estimated by the frequency of positive samples per group.

Flow cytofluorimetry. Spleen cells were double stained in suspension with anti-CD5 and anti-B220, anti-Ia and anti-CD8, or anti-CD4 (all from Gibco BRL, Gaithersburg, Md.) and anti-CD45RB monoclonal antibodies (MAbs) (clones 16A and 23G2) (PharMingen, San Diego, Calif.), labeled with phycoerythrin or fluorescein isothiocyanate. Stained cell suspensions were analyzed with a fluorescence-activated cell sorter (FACScan) (Becton Dickinson, Mountain View, Calif.) according to fluorescence intensity. $CD45RB^{High}$ and $CD45RB^{Low}$ subpopulations were analyzed from gated $CD4^+$ cells. Cell numbers in each subpopulation were then calculated from the total number of splenocytes. Blast cells from each subpopulation were determined by forward scatter (FSC) analysis of each gated region.

ELISASPOT for total isotype-specific immunoglobulin (Ig)-secreting cells. The ELISASPOT assay has been described in detail elsewhere (9, 38). In brief, 96-well flat-bottom MicroTest plates coated overnight (4°C) with goat anti-total mouse Ig (10 μg/ml) were saturated with 1% gelatin in phosphate-buffered saline for 60 min. Titrated spleen cells were added and cultured for 6 h in Dulbecco modified Eagle medium with 1% fetal calf serum. The spots were developed by adding goat anti-mouse IgM, IgG3, IgG1, IgG2b, or IgG2a biotinylated antibodies followed by a phosphatase alkaline-avidin conjugate (all antibodies and conjugates were obtained from Southern Biotechnology Associates, Birmingham, Ala.). 5-Bromo-4-chloro-3-indolylphosphate (BCIP) diluted in 2-amino-1-propanol buffer was used as substrate. From the titration plots (numbers of cells plated versus spots), the numbers of isotype-specific Ig-secreting cells in each cell suspension were calculated.

Cell culture conditions. Lymphoid cell suspensions were obtained from the spleens of individual mice. Dulbecco modified Eagle medium supplemented with 3% fetal calf serum and antibiotics was used as culture medium. Spleen cells (5×10^6/1-ml culture) were stimulated with 5 μg of concanavalin A (ConA; Sigma Chemical Co., St. Louis, Mo.) per ml. All cultures were incubated at 37°C in 5% CO_2 for 24 to 72 h. Culture supernatants were then harvested and frozen at −70°C until use.

ELISA for cytokines. Cytokines were quantified in culture supernatants from ConA-activated spleen cells by enzyme-linked immunosorbent assay (ELISA) (4). In brief, flat-bottom MicroTest plates were coated overnight (4°C) with either rat anti-IFN-γ, anti-IL-4, anti-IL-10, or anti-IL-2 MAbs and saturated with 1% gelatin for 1 h. Culture supernatants (50 μl/well) or standards at various concentrations were added and left for 2 h at room temperature. After extensive washing, a corresponding pair of biotinylated rat anticytokine MAbs diluted in phosphate-buffered saline–gelatin were added and incubated for 1 h at room temperature. The reaction was developed with peroxidase-conjugated streptavidin followed by *o*-phenylenediamine. The enzyme reaction was developed for 10 min and blocked with 3 N HCl (50 μl/well). A Dynatech reader with a 450-nm-wavelength filter quantified the absorbance values. Cytokine concentrations (nanograms per milliliter) were assigned to each experimental sample by using the linear part of recombinant cytokine standard curves (all antibodies and recombinants were obtained from PharMingen).

ELISA for parasite-specific antibodies. Serum anti-*T. cruzi* antibodies were quantified by ELISA. In brief, 96-well flat-bottom MicroTest plates were coated overnight (4°C) with a *T. cruzi* extract (50 μg/ml) obtained from the supernatant of tissue culture trypomastigotes of the Y strain subjected to several freeze-thawing cycles. Plates were saturated with 1% gelatin for 1 h. After washing, 50 μl of mouse serum samples (diluted 1/200 and 1/800 for IgM and IgG1 and diluted 1/3,200 and 1/25,600 for IgG2a) was added and left for 1 h at room temperature. A positive serum (hyperimmune serum) diluted from 1/100 to 1/51,200 was included in all the plates. The assays were developed by adding goat anti-mouse IgM, IgG1, or IgG2a biotinylated antibodies followed by a peroxidase-avidin conjugate and *o*-phenylenediamine. The enzyme reaction was developed for 10 min and blocked with 3 N HCl (50 μl/well). A Dynatech reader with a 450-nm-wavelength filter quantified the absorbance values. Antibody concentrations (micrograms per milliliter) of the IgG1 and IgG2a isotypes were estimated by indirect standardization (12), with slight modifications. In each ELISA plate, some of the wells were coated with anti-total mouse Ig (10 μg/ml) and incubated with serial dilutions of purified mouse Ig isotype standards (from 10 to 0.078 ng/well, in duplicate). The correspondence between optical density (OD) values and Ig isotype concentrations was established by the mathematical equation of the linear part of the Ig isotype standard curves. Parasite-specific antibody concentrations (micrograms per milliliter) of each serum were calculated by applying the OD values to this equation. Sample dilutions with OD values below or above the linear part of the hyperimmune serum curve were not considered. All antibodies, including conjugates and standards, were obtained from Southern Biotechnology Associates.

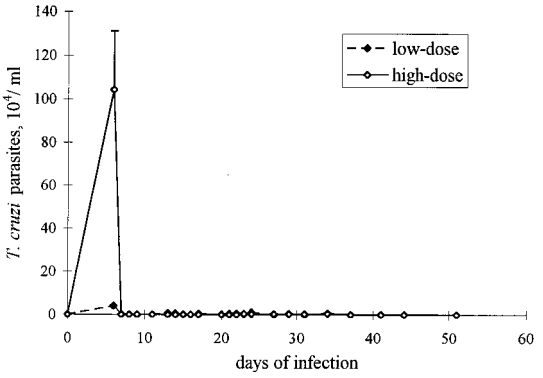

FIG. 1. Parasitemia curves of mice subjected to different parasite loads during the acute phase of *T. cruzi* infection. Mice were infected with 10^3 (low dose) or 10^5 (high dose) blood trypomastigotes and treated at day 6 with a single oral dose of benznidazole. Parasitemias were determined by direct examination of blood samples. Each point represents the mean ± standard deviation of individual values from six mice.

Histopathological analysis. Tissue specimens from chronically infected mice were collected and fixed in paraformaldehyde for further processing. Paraffin-embedded tissue sections were stained with hematoxylin-eosin and analyzed by optical microscopy. Six nonconsecutive slides from the heart and the quadriceps of each mouse were analyzed in a blind fashion. Areas of inflammatory infiltrates in the myocardium, pericardium, and endocardium or in the striated muscle were quantified by an image analysis system (Bioscan Optimas; Bioscan Inc., Edmonds, Wash.). The sum of infiltrated areas in the six slides was calculated for each mouse. The final individual score was expressed in square micrometers of inflammatory infiltrates per square millimeter of area examined.

Statistical analysis. The differences between the groups of mice used in this study were determined by Student's *t* test or the Mann-Whitney test.

RESULTS

Parasite load in the acute phase of *T. cruzi* infection. To obtain groups of infected mice with different parasite loads in the acute phase of the disease, mice were inoculated i.p. with 10^3 or 10^5 trypomastigotes and treated 6 days later with a single oral dose of benznidazole (200 mg/kg). Mice from the high-dose group showed 10^6 parasites/ml at day 6 (before the chemotherapy treatment), when low-dose-infected animals presented only 4×10^4 parasites/ml (Fig. 1). After chemotherapy, parasitemia dropped in both groups and parasites were only occasionally observed by optical microscopy.

Parasitemia levels in the chronic phase of *T. cruzi* infection. One year after infection, parasitemias of low-dose- and high-dose-infected mice were evaluated by a very sensitive semiquantitative subinoculation method that can detect as few as one circulating parasite (3). Mice infected with the high inoculum (10^5 parasites) showed higher parasitemia levels than those infected with the low parasite inoculum (10^3 parasites) (Table 1). Differences were evidenced by the numbers of chronically infected animals giving positive samples and by the percentage of positive samples in each group. In addition, when we considered only parasitemia-positive mice, 73.3% of blood transfusion samples from the high-dose group were positive compared to 48.1% in the low-dose group. These data suggest that parasitemia-positive mice from the high-dose group had more circulating parasites than parasitemia-positive animals from the low-dose group. Similar results were obtained when chronic-phase parasitemias were evaluated in mice infected with low and high inocula of CL strain trypomastigotes (data not shown).

TABLE 1. Parasitemia levels in the chronic phase of *T. cruzi* infection[a]

Expt no.	Chronic group[b]	No. of days of infection	% of chronically infected mice yielding positive samples (no. positive/total no.)	% of positive samples from total samples (no. positive/ total no.)
1	Low dose	315	41.66 (5/12)	19.44 (7/36)
	High dose	315	70.00 (7/10)	43.30 (13/ 30)
2	Low dose	326	42.85 (3/7)	19.04 (4/21)
	High dose	326	85.71 (6/7)	76.19 (16/ 21)
3	Low dose	476	20.00 (1/5)	13.33 (2/15)
	High dose	476	70.00 (7/10)	50.00 (15/ 30)

[a] Parasitemias were evaluated by a semiquantitative subinoculation method, in which 0.1-ml blood volumes from each chronically infected mouse were transfused into three native mice.

[b] Mice were infected with a low dose (10^3) or a high dose (10^5) of *T. cruzi* blood trypomastigotes, treated with benznidazole at day 6, and screened for parasitemias at the indicated times from the onset of infection.

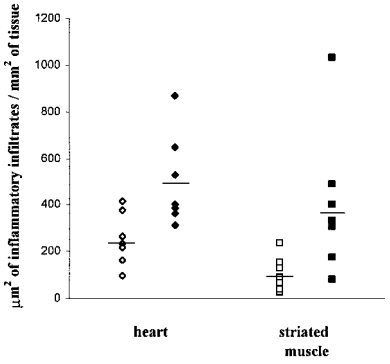

FIG. 2. Analysis of inflammatory infiltrates in the hearts and striated muscles of chronically infected mice subjected to different parasite loads at the acute phase of *T. cruzi* infection. Mice were infected with 10^3 (low dose; open symbols) or 10^5 (high dose; filled symbols) parasites and treated at day 6 with benznidazole. One year after infection, the infiltrated areas were quantified as described in Materials and Methods.

Histopathology of the hearts and striated muscles of chronically infected mice. High-dose-infected mice showed higher levels of myocarditis and myositis than low-dose-infected mice (Table 2 and Fig. 2). The greatest pathology was found in the hearts of quadriceps of mice from the high-dose group. Diffuse and focal infiltrates containing predominantly mononuclear cells were observed, some of the latter showing perivascular localization. Examples of mild focal, intermediate diffuse, and intense inflammatory foci are presented in Fig. 3. Higher numbers of degenerate fibers were also found in the striated muscles of the high-dose group. None of the infected mice presented parasite nests or showed severe pathology, conditions expected at the late chronic phase of the disease. Differences in the rates of endocarditis and pericarditis were not significant between the infected groups.

Analysis of lymphocyte populations in the spleens of chronically infected mice. The spleens of chronically infected mice were evaluated, since this is a major organ involved in parasite clearance. One year after infection, chronically infected animals contained two to three times more spleen cells than those of the control group. Among the infected animals, significant differences in spleen cellularity were observed between the low-dose ($[92.1 \pm 9.2] \times 10^6$) and high-dose ($[127.0 \pm 17.6] \times 10^6$) groups.

Regarding lymphocyte subpopulations, chronically infected mice showed decreased frequencies of $B220^+$ and $CD4^+$ cells, but not of $CD8^+$ cells, in relation to controls (Fig. 4A to C). When total spleen cell numbers were considered, however, all three lymphocyte populations were increased (Fig. 4G to I). Among the infected groups, significant differences in total lymphocyte numbers were observed only for the $CD8^+$ population, which was preferentially expanded in high-dose-infected mice. Increased frequencies of large cells from the three lymphocyte types were also observed in chronically infected mice, notably in the high-dose group (Fig. 4D to F). For large $CD8^+$ cells, however, differences between infected groups were not significant. Nevertheless, considering the total numbers of large cells per spleen, marked differences between the high- and low-dose groups for all three lymphocyte types were observed (Fig. 4G to I).

The drop in $B220^+$ and $CD4^+$ lymphocyte frequencies in the spleens of chronically infected mice resulted from the massive accumulation of a $B220^-$ $CD5^-$ $CD4^-$ $CD8^-$ population (Fig. 5). This population was preferentially augmented in the high-dose group, attaining frequencies above 30% (Fig. 5A). Many of these $B220^-$ $CD5^-$ cells were large in size and expressed class II molecules (Fig. 5C), FcγR, and high levels of Mac-1 (data not shown), suggestive of a macrophage phenotype. The frequencies of $B220^-$ $CD5^-$ cells in the spleens of infected mice, but not those of controls, correlated with the total spleen cellularity (correlation indices of −0.465, +0.852, and +0.733 for control, low-dose, and high-dose groups, respectively) (Fig. 5D). The total numbers of $B220^-$ $CD5^-$ cells in the spleens of high-dose-infected mice were 2.6 times greater than those of

TABLE 2. Heart and striated muscle pathology in chronically *T. cruzi*-infected mice

Chronic group[a]	Value for heart[b]				Value for striated muscle	
	Myocarditis	Endocarditis	Pericarditis	Total	Myositis[b]	Degenerate fibers[c]
Low dose	179.1 ± 117.6	18.7 ± 14.3	53.2 ± 51.1	251.7 ± 111.7	106.2 ± 72.4	5.1 ± 3.4
High dose	414.9 ± 169.9[d]	22.5 ± 22.4	62.7 ± 36.0	500.1 ± 199.0[d]	402.7 ± 309.3[d]	12.3 ± 8.6[d]

[a] Mice were infected with a low dose (10^3) or a high dose (10^5) of *T. cruzi* blood trypomastigotes, treated with benznidazole at day 6, and sacrified 1 year from the onset of the infection.

[b] Myocarditis, endocarditis, pericarditis, total heart infiltrates, and myositis are expressed as the means ± standard deviations of individual mouse data, in square micrometers of inflammatory infiltrates per square millimeter of heart or quadriceps examined.

[c] The incidence of degenerate fibers in the quadriceps is expressed as the means ± standard deviations of individual mouse data, in numbers of degenerate fibers per total area examined.

[d] $P < 0.05$ compared with the low-dose group (Mann-Whitney test; $n = 7$ mice per group).

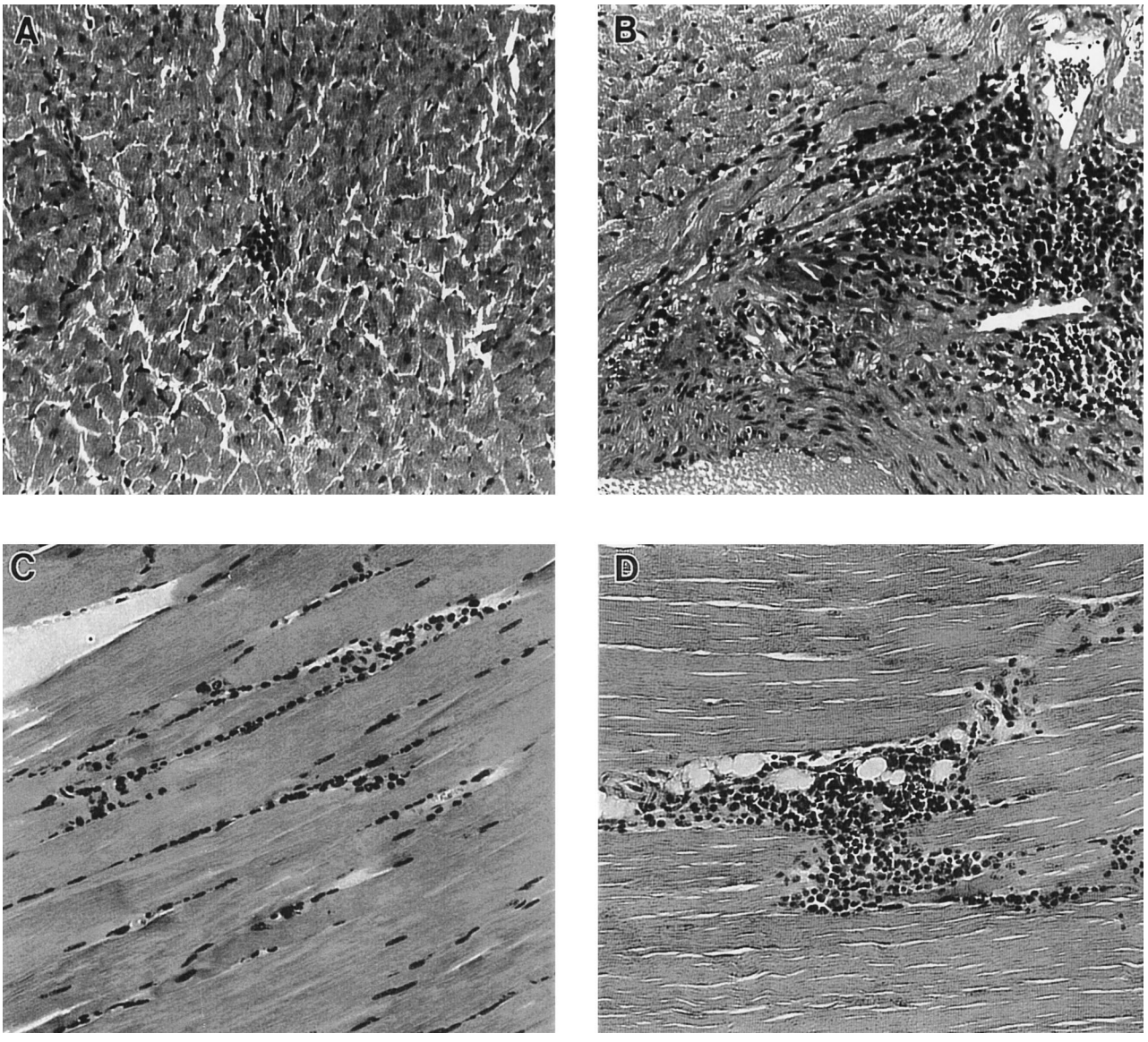

FIG. 3. Examples of lesions in the hearts and striated muscles (quadriceps) of mice infected with a low inoculum (10^3 parasites) or high inoculum (10^5 parasites) 1 year after infection. (A) Mild focal infiltrate in the left ventricle of a mouse infected with a low inoculum. (B) Intense ventricular infiltrate in a mouse infected with a high inoculum. (C and D) Moderate diffuse and intense focal infiltrates, respectively, in the quadriceps of mice infected with a high inoculum. Magnification, ×50.

low-dose-infected mice and 12.7 times greater than those of controls (Fig. 5B).

Expression of CD45RB by $CD4^+$ cells in the spleens of chronically infected mice. We analyzed the expression by $CD4^+$ cells of the CD45 tyrosine-phosphatase isoform CD45RB, which subdivides $CD4^+$ cells into a $CD45RB^{High}$ population, which includes naive and Th1 effector cells, and a $CD45RB^{Low}$ population, which includes experienced-memory cells and probably Th2 effector cells (5, 6, 20, 32). Our results, with the 16A MAb, showed that chronically infected mice from the high-dose group exhibited a shift towards the $CD4^+$ $CD45RB^{Low}$ phenotype (from 52.1% in the control group to 59.9% in the high-dose group) (Fig. 6A). Total $CD4^+$ $CD45RB^{Low}$ and $CD4^+$ $CD45RB^{High}$ cell numbers were augmented in the spleens of infected mice in relation to controls (Fig. 6C). When the infected groups were compared, total $CD4^+$ $CD45RB^{Low}$ cell numbers were augmented in mice from the high-dose group, whereas for $CD4^+$ $CD45RB^{High}$ cells no differences were observed between infected animals. Analysis of large cells from the $CD4^+$ $CD45RB^{High}$ and $CD4^+$ $CD45RB^{Low}$ phenotypes showed that chronically infected mice had increased frequencies of both phenotypes, notably those mice from the high-dose group (Fig. 6B). When the total numbers of large $CD4^+$ $CD45RB^{High}$ and $CD4^+$ $CD45RB^{Low}$ cells per spleen were considered, differences among the infected groups were even more pronounced (Fig. 6D). Interestingly, the ratio of $CD4^+$ $CD45RB^{Low}$ to $CD4^+$ $CD45RB^{High}$ large cells in the spleen did not change after *T. cruzi* infection. Results similar to those described here with the 16A MAb were obtained with the 23G2 MAb, which detects a different epitope of the CD45RB molecule (data not shown).

Analysis of antibody-producing cells in the spleens of chronically infected mice. Chronically infected mice, particularly those from the high-dose group, contained higher numbers of

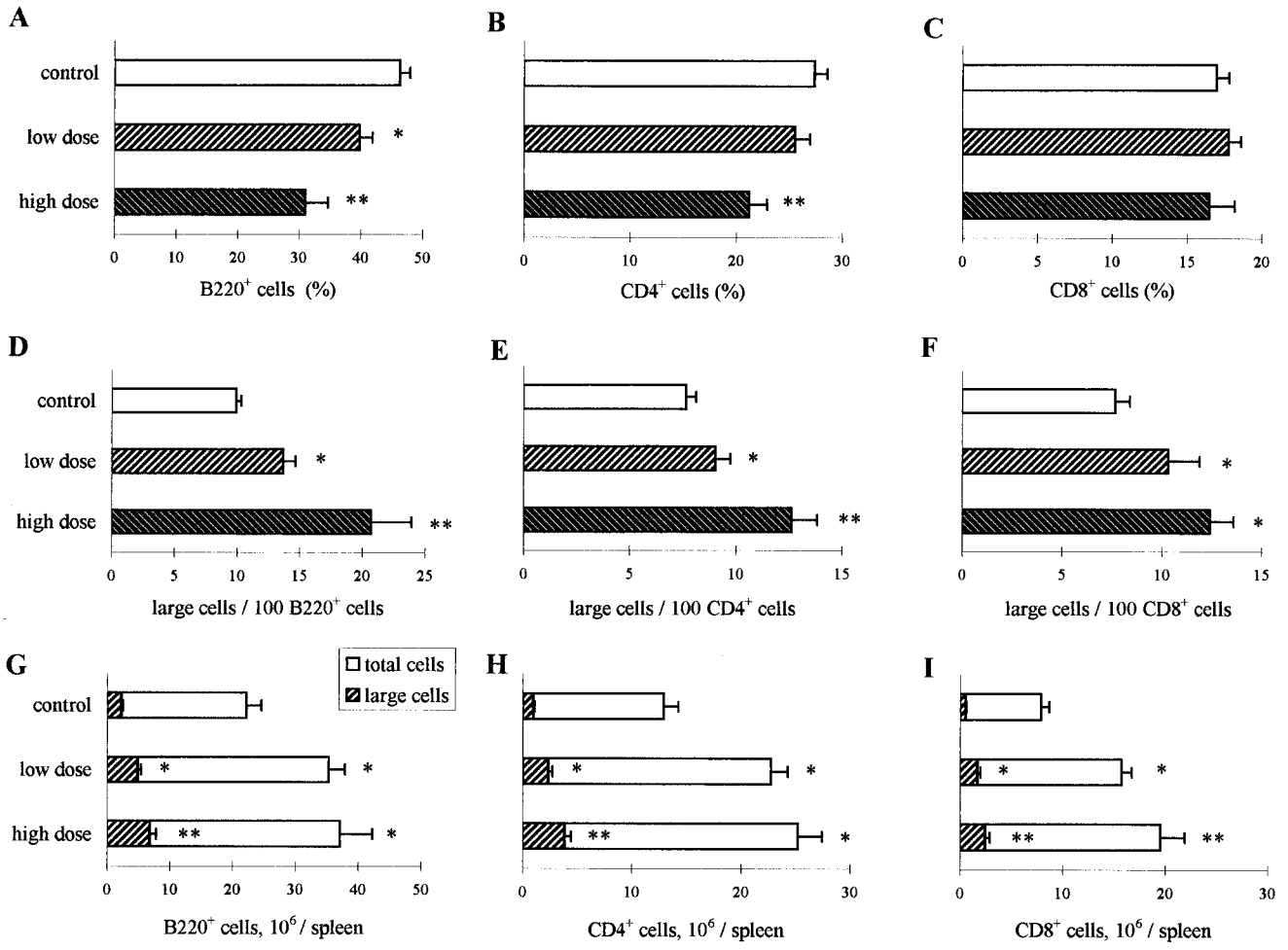

FIG. 4. Lymphocyte subpopulations in the spleens of chronically infected mice subjected to different parasite loads at the acute phase of *T. cruzi* infection. Mice were infected with 10^3 (low dose) or 10^5 (high dose) parasites and treated at day 6 with benznidazole. One year after infection, the frequencies of B ($B220^+$), $CD4^+$, and $CD8^+$ spleen cells were determined by fluorescence-activated cell sorting (A to C). Numbers of large cells were calculated by FSC analysis of gated lymphocyte populations (D to F). Numbers of total and large cells per spleen of each population were calculated by considering spleen cell numbers (G to I). Each bar represents the mean ± standard error of individual values from 10 or 11 mice. *, $P < 0.05$ compared with the control group; **, $P < 0.05$ compared with the control and the low-dose group.

Ig-producing cells than did control mice (Fig. 7). A switch to IgG characterized their Ig isotype distribution, with a predominance of IgG2a-secreting cells. High-dose-infected mice differed from low-dose-infected mice in total numbers of IgM-, IgG1-, and IgG2b-producing cells. Interestingly, the numbers of total Ig-producing cells of the IFN-γ-dependent isotypes IgG3 and IgG2a were not statistically different. Moreover, comparison of numbers of Ig-producing cells per 10^6 splenocytes revealed that IgG1, but not the other isotypes, was preferentially augmented in mice from the high-dose group (data not shown).

Analysis of parasite-specific serum antibodies of chronically infected mice. Analysis of parasite-specific antibodies in the serum of chronically infected mice showed high levels of IgM, IgG1, and IgG2a (Fig. 8) but low levels of IgG2b and IgG3 antibodies (data not shown). As observed for total Ig-producing cells in the spleen, the majority of anti-*T. cruzi* serum antibodies were from the IgG2a isotype. When infected groups were compared, the results revealed that mice from the high-dose group presented significantly lower levels of IgM and higher amounts of IgG1 and IgG2a antibodies in the serum. These results suggest that the increase of parasite load in the acute and/or chronic phases favored the switch of parasite-specific antibodies from IgM to IgG2a and IgG1.

Analysis of cytokine secretion in the spleens of chronically infected mice. Cytokine production by ConA-stimulated spleen cells from chronically infected mice was analyzed by ELISA. For all lymphokines, the results presented in Fig. 9 correspond to peak values obtained from 24-, 48-, or 72-h culture supernatants. High-dose-infected mice produced higher amounts of IFN-γ than did mice from the low-dose group (Fig. 9A). IL-4 was produced at low levels by infected and control groups (Fig. 9B). Production of this cytokine was also higher in the high-dose group than in the low-dose group, but it did not differ from that of controls. Indeed, IL-4 production by low-dose-infected mice was suppressed in relation to that of control mice, considering differences with $P < 0.1$. Correlation analysis of IL-4 and IFN-γ production in each mouse revealed that these cytokines do not segregate independently in the low- and high-dose groups. Moreover, when chronically infected mice were sorted by positive or negative parasitemias, a direct correlation between IL-4 and IFN-γ production was observed in

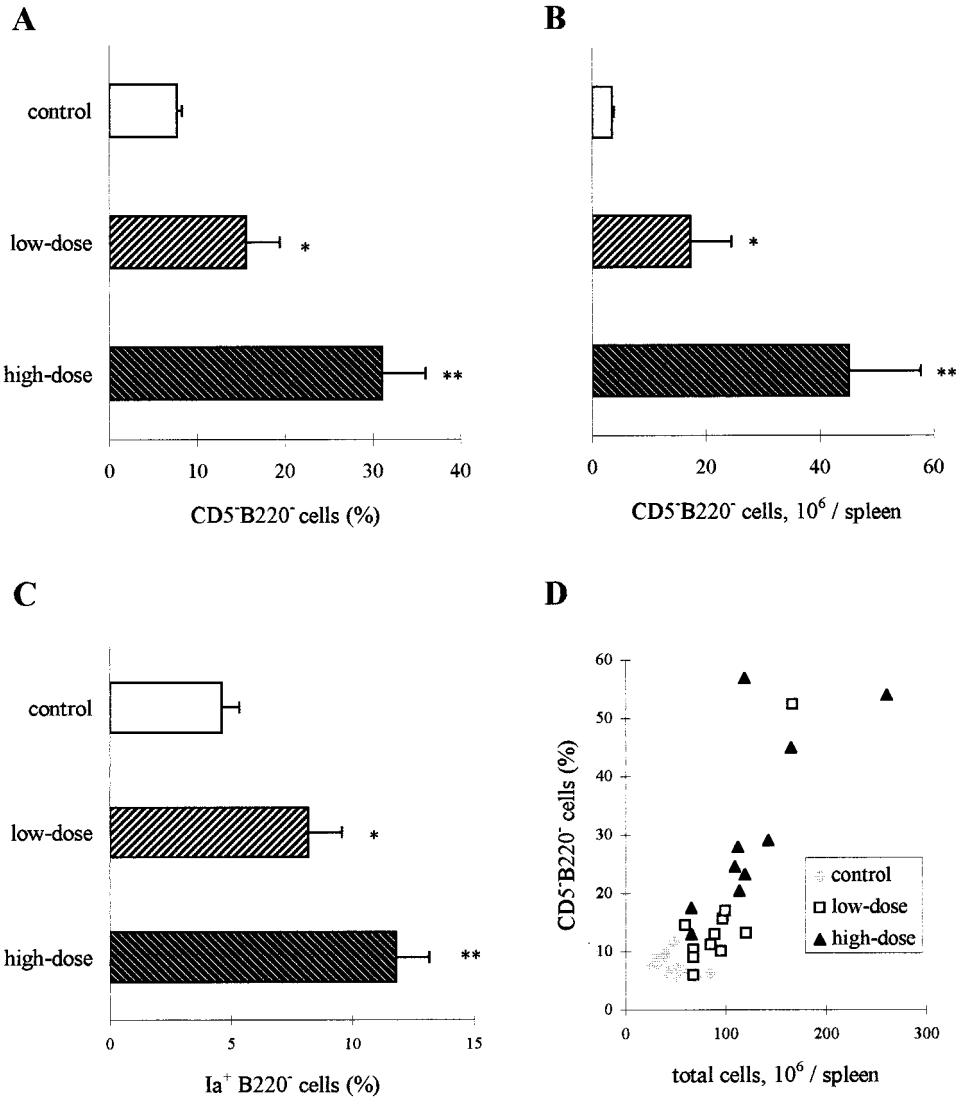

FIG. 5. Analysis of $CD5^-$ $B220^-$ cells in the spleens of chronically infected mice subjected to different parasite loads at the acute phase of *T. cruzi* infection. Mice were infected with 10^3 (low dose) or 10^5 (high dose) parasites and treated at day 6 with benznidazole. One year after infection, spleen cell suspensions were analyzed by fluorescence-activated cell sorting. (A) Frequency of $CD5^-$ $B220^-$ cells; (B) total numbers of $CD5^-$ $B220^-$ cells per spleen; (C) frequency of Ia^+ $B220^-$ cells; (D) correlation between frequencies of $CD5^-$ $B220^-$ cells and total numbers of spleen cells. Each bar represents the mean ± standard error of individual values from 10 or 11 mice. *, $P < 0.05$ compared with the control group; **, $P < 0.05$ compared with the control and the low-dose group.

parasitemia-positive mice (correlation index of 0.80) (Fig. 9E). For parasitemia-negative mice and controls, correlation indices were close to zero. These results indicate that chronically infected mice cannot be separated according to Th1 or Th2 phenotypes. Production of IL-2 was suppressed in both infected groups compared to controls (Fig. 9C). IL-10 secretion was higher in mice from the high-dose group, but data showed a high variability and the differences between the low- and high-dose groups were not significant (Fig. 9D). Nevertheless, when chronically infected mice were sorted by their parasitemias we observed that parasitemia-positive mice produced higher levels of IL-10 than did parasitemia-negative mice (Fig. 9F) ($P < 0.05$).

DISCUSSION

In this report, we show that the parasite load during the acute phase of *T. cruzi* infection directly correlates with the parasitemia, tissue pathology, and activation of the immune system at the late chronic phase of the disease. Thus, mice infected with a high inoculum showed, 1 year after infection, higher parasitemias than low-dose-infected mice. The increased parasitemias in the high-dose group could result either from a greater parasite input into the blood or from a less efficient removal of circulating parasites. The latter possibility is nevertheless unlikely, since the immune systems of high-dose-infected mice are more activated, presenting more effector molecules (e.g., IgG2a and IFN-γ) and cells (e.g., macrophages and $CD8^+$ cells) involved in parasite control. Therefore, the parasitemias exhibited by the low- and high-dose chronically infected mice must probably reflect the release of parasites from tissues into the blood and, indirectly, the levels of tissue parasitism. Inasmuch as tissue parasites in these groups remain different even after 1 year after the onset of the infection, we can consider that the immune effector

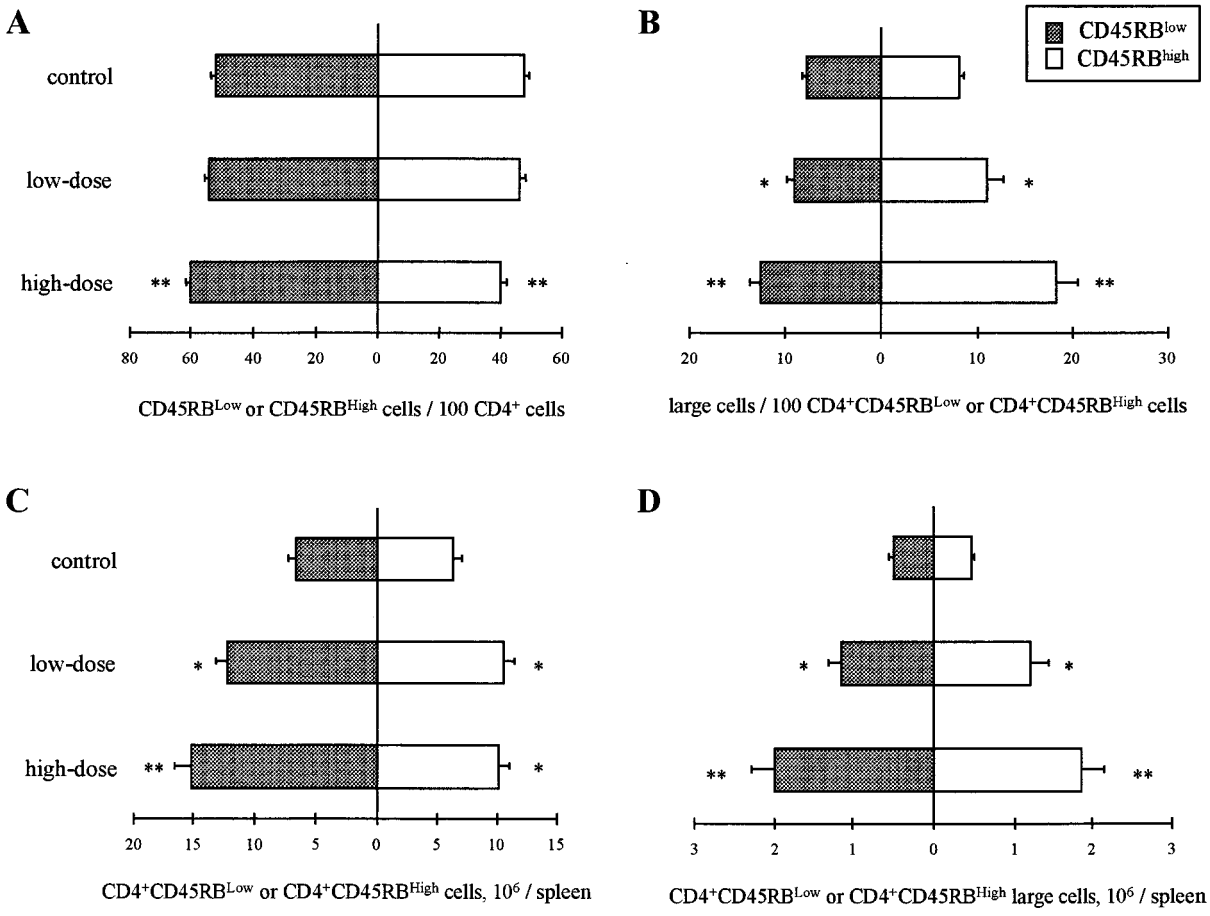

FIG. 6. CD45RB expression by $CD4^+$ spleen cells of chronically infected mice subjected to different parasite loads at the acute phase of *T. cruzi* infection. Mice were infected with 10^3 (low dose) or 10^5 (high dose) parasites and treated at day 6 with benznidazole. One year after infection, spleen cell suspensions were analyzed by fluorescence-activated cell sorting. (A) Frequencies of $CD45RB^{Low}$ and $CD45RB^{High}$ cells within $CD4^+$ lymphocytes; (B) frequencies of large cells in the $CD4^+$ $CD45RB^{Low}$ and $CD4^+$ $CD45RB^{High}$ subsets calculated by FSC analysis of each gated subpopulation; (C) total numbers of $CD4^+$ $CD45RB^{Low}$ and $CD4^+$ $CD45RB^{High}$ cells per spleen; (D) total numbers of $CD4^+$ $CD45RB^{Low}$ and $CD4^+$ $CD45RB^{High}$ large cells per spleen. Each bar represents the mean ± standard error of individual values from 10 or 11 mice. *, $P < 0.05$ compared with the control group; **, $P < 0.05$ compared with the control and the low-dose group.

mechanisms are not very efficient in controlling tissue parasite growth.

In the hearts or striated muscles, inflammatory infiltrates and degenerate fibers were clearly more evident in mice from the high-dose group. These data indicate that the parasite load during the acute phase influences the intensity of pathology at the chronic phase of the disease. Thus, control of the parasite load during the acute phase, which is dependent on the genetic background of the host (21) and of the parasite itself (30), is directly related to the pathology observed at the chronic phase. These findings have important implications for the prevention of Chagas' disease pathology, reinforcing the need for chemotherapy at the early phase of infection. The increased tissue inflammatory reactions in the high-dose group also reinforce the idea that these mice present a higher tissue parasitism. Although we did not detect parasite nests in the hearts or striated muscles, this idea is indirectly supported by data showing, in chronic Chagas' disease patients, a positive correlation between parasitism and pathology (15, 17, 46). Moreover, the reported lower incidence of pathology after chemotherapy in the chronic phase of the disease is suggestive of this correlation (39, 48).

The parasite load in the acute phase of infection correlates, at the late chronic phase, with the intensity of activation of the immune system. According to various immunological parameters, spleen cells from high-dose-infected mice were more activated than those from mice of the low-dose group. Thus, chronically infected mice infected with the high parasite inoculum presented (i) increased numbers of splenocytes, with preferential expansion of $CD8^+$ and accumulation of $B220^-$ $CD5^-$ cells, many of them bearing a macrophage phenotype; (ii) higher frequencies of $B220^+$, $CD4^+$, and $CD8^+$ large lymphocytes; (iii) a shift of $CD4^+$ cells towards a $CD45RB^{Low}$ phenotype, suggesting an increase of memory-experienced T cells; (iv) increased frequencies of $CD45RB^{Low}$ and $CD45RB^{High}$ large $CD4^+$ cells; (v) augmented numbers of total Ig-secreting cells, characterized by the predominance of IgG2a antibodies; and (vi) increased production of IFN-γ and IL-4. In addition, regarding parasite-specific antibodies, these animals presented lower IgM and higher IgG2a and IgG1 serum levels. Nevertheless, production of IL-2 was reduced to low levels in both infected groups, confirming previous observations of suppressed in vitro and in vivo secretion of this cytokine in the acute and chronic phases (8, 14, 49).

One interesting finding in this work was the accumulation of $B220^-$ $CD5^-$ cells in the spleens of infected animals, notably in mice from the high-dose group. Many of these cells seemed to be macrophages because of their large size and Ia, FcR, and

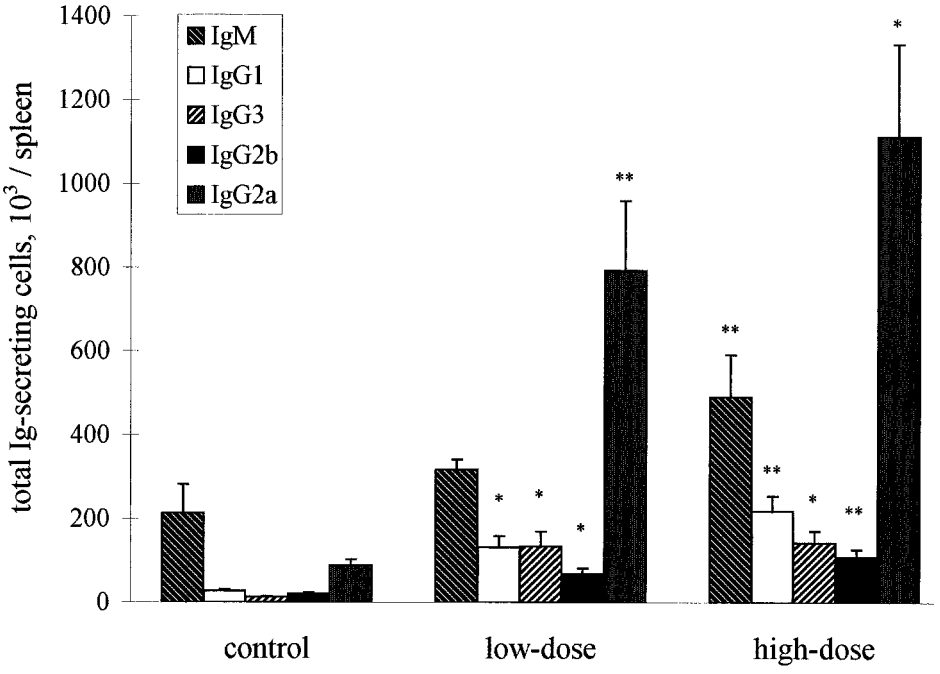

FIG. 7. Total Ig-secreting cells in the spleens of chronically infected mice subjected to different parasite loads at the acute phase of *T. cruzi* infection. Mice were infected with 10^3 (low dose) or 10^5 (high dose) parasites and treated at day 6 with benznidazole. One year after infection, spleen cell suspensions were analyzed by ELISASPOT to determine the numbers of Ig-secreting cells of the different isotypes. Each bar represents the mean ± standard error of individual values from 10 or 11 mice. *, $P < 0.05$ compared with the control group; **, $P < 0.05$ compared with the control and the low-dose group.

high Mac-1 expression (data not shown). Macrophages have been shown to be essential for *T. cruzi* blood and tissue clearances, working in conjunction with opsonizing IgG2a antibodies. Moreover, macrophages are also crucial for intracellular *T. cruzi* destruction, a process that for reticulotropic parasites is critically dependent on macrophage activation by cytokines, such as IFN-γ, tumor necrosis factor, and granulocyte-macrophage colony-stimulating factor (1, 2, 27–29, 37), and that is subjected to down-regulation by IL-10 and transforming growth factor β (13, 40). In this respect, it is noticeable that in our experiments high production of IL-10, a cytokine secreted by macrophages, Th2 lymphocytes, and other cells (25, 26), was restricted to parasitemia-positive mice, with very low production by chronically infected mice with negative parasitemias. IL-10 has been shown to down-regulate immune responses that are detrimental for the host (19). Nevertheless, because of its macrophage-deactivating activity, this cytokine could play a key countereffector role in the chronic phase of *T. cruzi* infection, reducing the control of circulating parasites (1, 16).

In relation to controls, $CD8^+$ cells were among those spleen

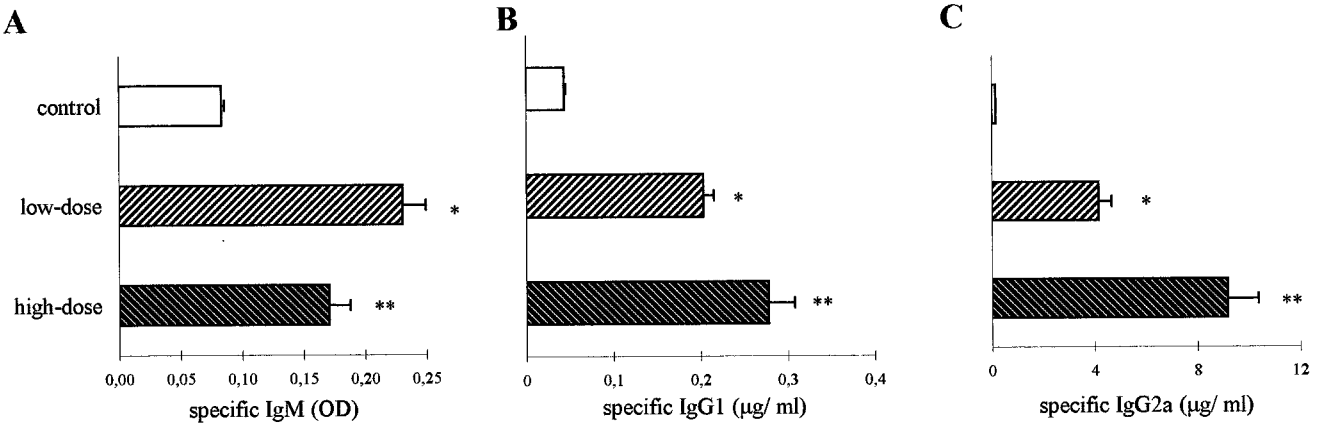

FIG. 8. Parasite-specific antibodies in the serum of chronically infected mice subjected to different parasite loads at the acute phase of *T. cruzi* infection. Mice were infected with 10^3 (low dose) or 10^5 (high dose) parasites and treated at day 6 with benznidazole. One year after infection, mice were bled and their sera were analyzed by ELISA to determine the levels of specific IgM (A), IgG1 (B), and IgG2a (C) antibodies. Concentrations (micrograms per milliliter) of specific IgG1 and IgG2a were calculated from standard curves as described in Materials and Methods. Levels of specific IgM are expressed as OD of serum samples diluted 1/800. Each bar represents the mean ± standard error of individual values from 10 or 11 mice. *, $P < 0.05$ compared with the control group; **, $P < 0.05$ compared with the control and the low-dose group.

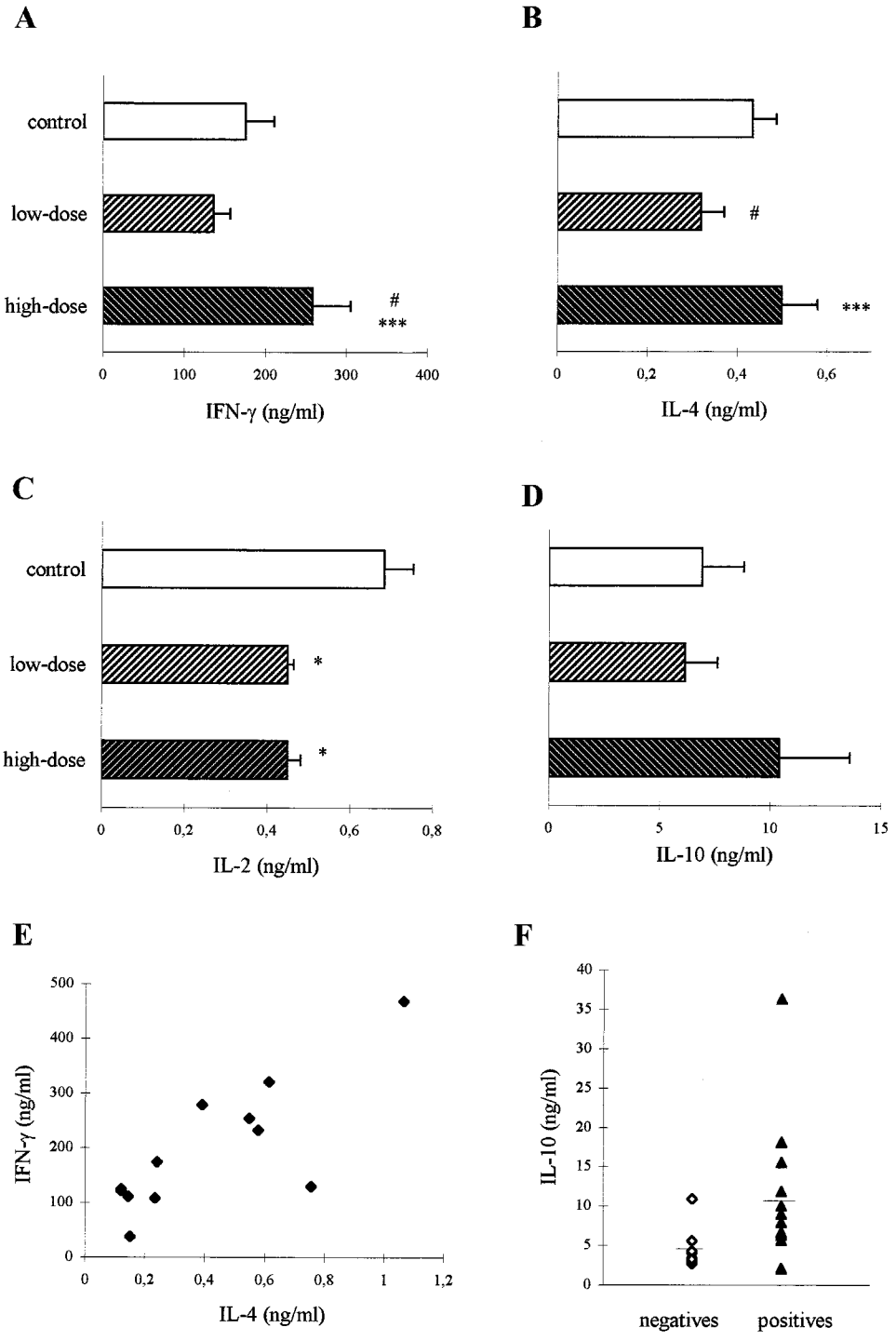

FIG. 9. Cytokine production in ConA-stimulated cultures of splenocytes from chronically infected mice subjected to different parasite loads at the acute phase of *T. cruzi* infection. Mice were infected with 10^3 (low dose) or 10^5 (high dose) parasites and treated at day 6 with benznidazole. One year after infection, spleen cell suspensions were cultured with ConA, and the 24- to 72-h supernatants were tested by capture ELISA. (A to D) Peak production for IFN-γ (A), IL-4 (B), IL-2 (C), and IL-10 (D). (E) Correlation between IFN-γ and IL-4 production by parasitemia-positive chronically infected mice. (F) IL-10 production by parasitemia-negative and -positive mice. Each bar represents the mean ± standard error of individual values from 10 or 11 mice. *, $P < 0.05$ compared with the control group; #, $P < 0.1$ compared with the control group; ***, $P < 0.05$ compared with the low-dose group.

lymphocytes preferentially expanded in chronically infected mice. Moreover, differences between the infected groups were observed only for this population, with increased numbers in the high-dose group. $CD8^+$ lymphocytes are important effector cells in *T. cruzi* parasite control, since acutely infected mice lacking these cells presented increased parasitemias (34, 43). Their expansion in the spleen, a major organ for trypomastigote clearance, could have a significant role in the destruction

of nonactivated or deactivated infected macrophages permissive for parasite growth. Moreover, recognition by $CD8^+$ cells of *T. cruzi* epitopes in class I molecules of infected macrophages could induce the production of IFN-γ, which in turn would promote the intracellular killing of the amastigotes. Spleen $CD8^+$ cells could be essential in the control of reticulotropic parasites, since these parasites can easily proliferate inside macrophages, unless they are activated.

Chronically infected mice infected with low and high parasite inocula presented a preferential production of IFN-γ-dependent IgG2a antibodies, revealed by the total spleen numbers of Ig-producing cells and by the levels of anti-*T. cruzi* antibodies in serum. Among the infected groups, only minor differences in terms of the Ig isotype distribution were observed. Previous studies showed that IgG2a is the major isotype secreted in the acute infection and at the early chronic phase of the disease (10, 11). The increased production of IgG2a 1 year after *T. cruzi* infection suggests that the Th1 pattern of the immune response predominates during the whole course of the disease. In spite of that, our data suggest that chronically infected mice also presented activated Th2 cells. Interestingly, similarly to the Th1 response, Th2 activation was more intensive in mice from the high-dose group. Thus, these animals showed (i) increased frequencies of IgG1-secreting cells in the spleen; (ii) high levels of parasite-specific IgG1 serum antibodies; (iii) high spleen numbers of $CD4^+$ $CD45RB^{Low}$ large cells; and (iv) IL-4 production, not different from controls, but significantly higher than that observed in low-dose-infected mice. Production of IL-4 by spleen cells in late chronic disease was also observed by Zhang and Tarleton (49). Interestingly, correlation analysis of IL-4 and IFN-γ production in each mouse revealed that these cytokines do not segregate independently in chronically infected animals. Moreover, the direct correlation observed between IL-4 and IFN-γ production in parasitemia-positive mice suggests that Th2 activation follows IFN-γ secretion. These results suggest that in chronically infected mice signaling for IL-4 also depends on the parasite load and may result from presentation of *T. cruzi* antigens by different antigen-presenting cells than those involved in danger signaling and/or from homeostatic control mechanisms counterbalancing Th1 polarization. In this respect, it is interesting that similar ratios of $CD4^+$ $CD45RB^{Low}$ and $CD4^+$ $CD45RB^{High}$ large cells were observed in mice from both chronically infected groups and from the control group, which could suggest that the immune systems of chronically infected mice tend toward equilibrium independently of the levels of circulating parasites. $CD4^+$ $CD45RB^{High}$ cells have been shown to present an autoaggressive behavior, mediating multiple organ pathology and wasting disease, which is prevented by $CD4^+$ $CD45RB^{Low}$ cells (31).

The results presented here show that the parasite load during the acute phase of *T. cruzi* infection affects the parasitemia, pathology, and immune response at the late chronic phase of the disease. This study may suggest the perspective that therapeutic protocols that control the parasite load could reduce chronic Chagas' disease pathology.

ACKNOWLEDGMENTS

This work was supported by grants from Fundação de Amparo à Pesquisa do Estado de São Paulo (Brazil).

We thank Irene Simphonio and Paulo Abe for technical assistance, the Laboratory of Transplant Immunology of the São Paulo Medical School for use of the FACScan, Paulo Abrahamson and José L. Guerra for help in software analysis of pathology data, and Ises Abrahamson and Momtchilo Russo for helpful discussion and revision of the manuscript.

REFERENCES

1. **Abrahamsohn, I. A., and R. L. Coffman.** 1996. *Trypanosoma cruzi*: IL-10, TNF, IFN-gamma, and IL-12 regulate innate and acquired immunity to infection. Exp. Parasitol. **84:**231–244.
2. **Aliberti, J. C., M. A. Cardoso, G. A. Martins, R. T. Gazzinelli, L. Y. Vieira, and J. S. Silva.** 1996. Interleukin-12 mediates resistance to *Trypanosoma cruzi* in mice and is produced by murine macrophages in response to live trypomastigotes. Infect. Immun. **64:**1961–1967.
3. **Alvarez, J. M., A. Oshima, V. Mozer, and L. Guimarães.** 1991. Evolution of subpatent parasitaemia in *Trypanosoma cruzi* chronically infected mice with the help of a cyclophosphamide amplification transfer assay. Rev. Inst. Med. Trop. São Paulo **33:**509–514.
4. **Avrameas, S., T. Ternynck, and J. L. Guesdon.** 1979. Coupling of enzymes to antibodies and antigens. Scand. J. Immunol. **8:**7–23.
5. **Birkeland, M. L., P. Johnson, I. S. Trowbridge, and E. Puré.** 1989. Changes in CD45 isoform expression accompany antigen-induced murine T-cell activation. Proc. Natl. Acad. Sci. USA **86:**6734–6738.
6. **Bottomly, K., M. Luqman, L. Greenbaum, S. Carding, J. West, T. Pasqualini, and D. B. Murphy.** 1989. A monoclonal antibody to murine CD45R distinguishes CD4 T cell populations that produce different cytokines. Eur. J. Immunol. **19:**617–623.
7. **Cunha-Neto, E., M. Duranti, A. Gruber, B. Zingales, I. De Messias, N. Stolf, G. Bellotti, M. E. Patarroyo, F. Pilleggi, and J. Kalil.** 1995. Autoimmunity in Chagas disease cardiopathy: biological relevance of a myosin-specific epitope cross-reactive to an immunodominant *Trypanosoma cruzi* antigen. Proc. Natl. Acad. Sci. USA **92:**3541–3545.
8. **Curotto de Lafaille, M. A., L. C. Barbosa de Oliveira, G. C. Lima, and I. Abrahamsohn.** 1990. *Trypanosoma cruzi*: maintenance of parasite-specific T cell responses in lymph nodes during the acute phase of the infection. Exp. Parasitol. **70:**164–174.
9. **Czerkinsky, C. C., L. A. Nilsson, H. Nygren, O. Ouchterlony, and A. Tarkowski.** 1983. A solid phase immunoenzymatic technique for the enumeration of specific antibody-secreting cells. J. Immunol. Methods **65:**109–121.
10. **D'Império Lima, M. R., H. Eisen, P. Minóprio, M. Joskowicz, and A. Coutinho.** 1986. Persistence of polyclonal B cell activation with undetectable parasitemia in late stages of experimental Chagas' disease. J. Immunol. **137:**353–357.
11. **D'Império Lima, M. R., M. Joskowicz, A. Coutinho, T. Kipnis, and H. Eisen.** 1985. Very large and isotypically atypical polyclonal plaque forming cell responses in mice infected with *Trypanosoma cruzi*. Eur. J. Immunol. **15:**201–203.
12. **Ferreira, M. U., E. A. S. Kimura, J. M. Souza, and A. M. Katzin.** 1996. The isotype composition and avidity of naturally acquired anti-*Plasmodium falciparum* antibodies: differential patterns in clinically immune Africans and Amazonian patients. Am. J. Trop. Med. Hyg. **55:**315–323.
13. **Gazzinelli, R. T., I. P. Oswald, S. Hieny, S. L. James, and A. Sher.** 1992. The microbicidal activity of interferon-gamma-treated macrophages against *Trypanosoma cruzi* involves an L-arginine-dependent, nitrogen oxide mediated mechanism inhibitable by interleukin-10 and transforming growth factor-beta. Eur. J. Immunol. **22:**2501–2506.
14. **Harel-Bellan, A. M., M. Joskowicz, D. Fradelizi, and H. Eisen.** 1983. Modification of T cell proliferation and interleukin-2 production in mice infected with *Trypanosoma cruzi*. Proc. Natl. Acad. Sci. USA **80:**3466–3469.
15. **Higuchi, M., T. De Brito, M. M. Reis, A. Barbosa, G. Bellotti, A. C. Pereira-Barreto, and F. Pileggi.** 1993. Correlation between *Trypanosoma cruzi* parasitism and myocardial inflammatory infiltrate in human chronic chagasic myocarditis: light microscopy and immunohistochemical findings. Card. Pathol. **2:**101–106.
16. **Hunter, C. A., L. A. Ellis-Neyes, T. Slifer, S. Kanaly, G. Grunig, M. Fort, D. Rennick, and F. G. Araujo.** 1997. IL-10 is required to prevent immune hyperactivity during infection with *Trypanosoma cruzi*. J. Immunol. **158:**3311–3316.
17. **Jones, E. M., D. G. Colley, S. Tostes, E. Reis Lopes, C. L. Vnencak-Jones, and T. L. McCurley.** 1993. Amplification of a Trypanosoma cruzi DNA sequence from inflammatory lesions in human chagasic cardiomyopathy. Am. J. Trop. Med. Hyg. **48:**348–357.
18. **Krettli, A. U., and Z. Brenner.** 1976. Protective effects of specific antibodies in *Trypanosoma cruzi* infection. J. Immunol. **116:**755–760.
19. **Kühn, R., J. Löhler, D. Rennick, K. Rajewski, and W. Müller.** 1993. Interleukin-10 deficient mice develop chronic enterocolitis. Cell **75:**203–274.
20. **Lee, W. T., X. M. Yin, and E. S. Vitetta.** 1990. Functional and ontogenic analysis of murine $CD45^{hi}$ and $CD45^{lo}$ $CD4^+$ T cells. J. Immunol. **144:**3288–3295.
21. **Llop, F., F. Rothhammer, M. Acuna, and W. Apt.** 1988. HLA antigens in cardiomyopathic Chilean chagasics. Am. J. Hum. Genet. **43:**770–773.
22. **Minóprio, P., A. Bandeira, P. Pereira, T. A. Mota-Santos, and A. Coutinho.** 1989. Preferential expansion of Ly1-B and CD4−CD8− T cells in the polyclonal lymphocyte responses to murine *Trypanosoma cruzi* infection. Int. Immunol. **1:**176–184.
23. **Minóprio, P., L. Andrade, M. P. Lembezat, L. S. Ozaki, and A. Coutinho.** 1989. Indiscriminate representation of VH-gene families in the murine B

lymphocyte responses to *Trypanosoma cruzi*. J. Immunol. **142:**4017–4021.
24. **Moncayo, A.** 1993. Maladie de Chagas. WHO/TDR Program Rep. **11:**67.
25. **Mosmann, T. R., and K. W. M. Moore.** 1991. The role of IL-10 in cross-regulation of Th1 and Th2 responses. Immunol. Today **12:**49–53.
26. **Mosmann, T. R., J. H. Schumaker, N. F. Street, R. Budd, A. O'Garra, T. A. T. Fong, M. W. Bond, K. W. M. Moore, A. Sher, and D. F. Fiorentino.** 1991. Diversity of cytokine synthesis and function of mouse $CD4^+$ T cells. Immunol. Rev. **123:**209–229.
27. **Muñoz-Fernandez, M. A., M. A. Fernandez, and M. Fresno.** 1992. Synergism between tumor necrosis factor-alpha and interferon-gamma on macrophage activation for the killing of intracellular *Trypanosoma cruzi* through a nitric oxide-dependent mechanism. Eur. J. Immunol. **22:**301–307.
28. **Olivares-Fontt, E., K. Heirman, K. Thielemans, and B. Vray.** 1996. Granulocyte-macrophage colony-stimulating factor: involvement in control of *Trypanosoma cruzi* infection in mice. Infect. Immun. **64:**3429–3434.
29. **Petray, P. B., M. E. Rottemberg, G. Bertot, R. S. Corral, A. Diaz, A. Örn, and S. Gristein.** 1993. Effect of anti-γ-interferon and anti-interleukin-4 administration on the resistance of mice against infection with reticulotropic and myotropic strains of *Trypanosoma cruzi*. Immunol. Lett. **35:**77–80.
30. **Postan, M., J. J. Bailey, J. A. Dvorak, J. P. McDaniel, and E. W. Pottala.** 1987. Studies of *Trypanosoma cruzi* clones in inbred mice. III. Histopathological and electrocardiographical responses to chronic infection. Am. J. Trop. Med. Hyg. **37:**541–549.
31. **Powrie, F., and D. Mason.** 1990. $Ox\text{-}22^{High}$ $CD4^+$ T cells induce wasting disease with multiple organ pathology: prevention by the $Ox\text{-}22^{Low}$ subset. J. Exp. Med. **172:**1701–1708.
32. **Powrie, F., R. Correa-Oliveira, S. Mauze, and R. L. Coffman.** 1994. Regulatory interactions between $CD45RB^{High}$ and $CD45RB^{Low}$ cells are important for the balance between protective and pathologic cell-mediated immunity. J. Exp. Med. **179:**589–600.
33. **Rodriguez, A. M., F. Santoro, D. Afchain, H. Bazin, and A. Capron.** 1981. *Trypanosoma cruzi* infection in B-cell-deficient rats. Infect. Immun. **31:**524–529.
34. **Rottemberg, M. E., A. Riarte, L. Sporrong, J. Alcheh, P. Petray, A. M. Ruiz, H. Wigzell, and A. Orn.** 1995. Outcome of infection with different strains of *Trypanosoma cruzi* in mice lacking CD4 and/or CD8. Immunol. Lett. **45:**53–60.
35. **Russo, M., N. Starobinas, P. Minóprio, A. Coutinho, and M. Hontebeyrie-Joskowicz.** 1988. Parasitic load increases and myocardial inflammation decreases in *Trypanosoma cruzi*-infected mice after activation of helper T cells. Ann. Inst. Pasteur Immunol. **139:**225–236.
36. **Sadigursky, M., A. M. Acosta, and C. A. Santos-Busch.** 1982. Muscle sarcoplasmic reticulum antigen shared by a *Trypanosoma cruzi* clone. Am. Soc. Trop. Med. Hyg. **31:**934–941.
37. **Santos-Lima, E. C., I. Gracia, M. H. Vicentelli, P. Vassalli, and P. Minóprio.** 1997. Evidence for a protective role of tumor necrosis factor in the acute phase of *Trypanosoma cruzi* infection in mice. Infect. Immun. **65:**457–465.
38. **Sedgwick, J. D., and P. G. Holt.** 1983. A solid-phase immunoenzymatic technique for enumeration of specific antibody-secreting cells. J. Immunol. Methods **57:**301–309.
39. **Segura, M. A., E. Moline de Raspi, and M. A. Basombrio.** 1994. Reversibility of muscle and heart lesions in chronic *T. cruzi* infected mice after late trypanocidal treatment. Mem. Inst. Oswaldo Cruz **89:**213–216.
40. **Silva, J. S., D. R. Twardzik, and S. J. Reed.** 1991. Regulation of *Trypanosoma cruzi* infections *in vitro* and *in vivo* by transforming growth factor beta (TGF beta). J. Exp. Med. **174:**539–545.
41. **Tarleton, R. L.** 1990. Depletion of $CD8^+$ cells increases susceptibility and reverses vaccine-induced immunity in mice infected with *Trypanosoma cruzi*. J. Immunol. **144:**717–724.
42. **Tarleton, R. L.** 1993. Pathology of American trypanosomiasis, p. 64–71. *In* K. S. Warren (ed.), Immunology and molecular biology of parasitic infections, 3rd ed. Blackwell Scientific Publications, Boston, Mass.
43. **Tarleton, R. L., B. H. Koller, A. Latour, and M. Postan.** 1992. Susceptibility of β2 microglobulin-deficient mice to *Trypanosoma cruzi* infection. Nature **356:**338–340.
44. **Tarleton, R. L., L. Zhang, and M. O. Downs.** 1997. "Autoimmune rejection" of neonatal heart transplants in experimental Chagas disease is a parasite-specific response to infected host tissue. Proc. Natl. Acad. Sci. USA **94:**3932–3937.
45. **Torrico, F., H. Heremans, M. T. Rivera, E. Van Marck, A. Billiau, and Y. Carlier.** 1991. Endogenous IFN-gamma is required for resistance to acute *Trypanosoma cruzi* infection in mice. J. Immunol. **146:**3626–3632.
46. **Vago, A. R., A. M. Macedo, S. J. Adad, D. D'Avila Reis, and R. Correia de Oliveira.** 1996. PCR detection of *Trypanosoma cruzi* DNA in oesophageal tissue of patients with chronic digestive Chagas' disease. Lancet **348:**891–892.
47. **Van Voorhis, W. C., and H. Eisen.** 1989. FL160. A surface antigen of *Trypanosoma cruzi* that mimics mammalian nervous tissue. J. Exp. Med. **169:**641–652.
48. **Viotti, R., C. Vigliano, H. Armeti, and E. Segura.** 1994. Treatment of chronic Chagas' disease with benzonidazole: clinical and serological evolution of patients with long-term follow-up. Am. Heart J. **127:**151–162.
49. **Zhang, L., and R. L. Tarleton.** 1996. Characterization of cytokine production in murine *Trypanosoma cruzi* infection by in situ immunocytochemistry: lack of association between susceptibility and type 2 cytokine production. Eur. J. Immunol. **26:**102–109.

Editor: S. H. E. Kaufmann